Composite Structures 229 (2019) 111400

Contents lists available at ScienceDirect

Composite Structures

journal homepage: www.elsevier.com/locate/compstruct

Hybrid fiber use on flexural behavior of ultra high performance fiber reinforced concrete beams

Kaan Turker[a,*], Umut Hasgul[a], Tamer Birol[a], Altug Yavas[a], Halit Yazici[b]

[a] Department of Civil Engineering, Engineering Faculty, Balikesir University, Turkey
[b] Department of Civil Engineering, Engineering Faculty, Dokuz Eylul University, Turkey

ARTICLE INFO

Keywords:
Ultra-high performance fiber reinforced concrete
RC beam
Flexural behavior
Hybrid fiber

ABSTRACT

In this study, the flexural behavior of Ultra-High Performance Fiber Reinforced Concrete (UHPFRC) beams produced in mono and hybrid forms were investigated experimentally and numerically. Twelve doubly reinforced concrete beams were casted with four different reinforcement ratios representing low to excessive levels. The beams were produced in three groups to study the effects of mono and hybrid steel fiber usages. The first group beams of four are non-fiber beams while the second group contains only short-straight fiber of 13 mm. The last group is composed of hybrid form where the short-straight fiber of 13 mm and the long-hooked fiber of 60 mm were blended together. The beams were subjected to four-point loading, and the parameters of deflection and curvature ductilities, flexural stiffness, flexural moment capacity, cracking behavior and compressive strain were discussed. The test results indicated that the UHPFRC beams with high reinforcement ratios above the limits in current design codes provide remarkable benefits through the fibers' contribution. It can be deduced that the hybrid fiber usage showed better flexural performance, in general, comparing to the mono form. In addition, two numerical approaches were proposed to predict nominal moment capacity of the UHPFRC beams in the mono or hybrid form.

1. Introduction

Over the last two decades, the production of Ultra-High Performance Fiber Reinforced Concrete (UHPFRC) has become possible with the new developments in concrete technology. The term UHPFRC is commonly used when the concrete compressive strength exceeds 150 MPa and strain-hardening response is ensured with sufficient fiber content. When compared to normal and high strength concrete, the UHPFRC has excellent compressive and tensile strength, high deformation capacity as well as durability and long-term stability through high density matrix, very low water/binder ratio and special treatments such as curing under heat/pressure. However, tensile properties of the UHPFRC are distinct from others in consequence of the post-cracking capacity of concrete matrix and the crack bridging behavior of steel fibers [1]. Thus, the UHPFRC provides various advantages over the conventional non-fiber and fibrous concrete such as higher ductility and strength.

The use of UHPFRC in various structural applications including industrial structures, bridges, viaducts, piers, impact-resistant structures as well as repairing and strengthening works has attracted high interest from the research community [2–4]. Beside the compressive strength of UHPFRC is much greater than that of the conventional concrete, its high elastic modulus permits use of members having smaller cross-sectional dimensions. Also, higher flexural and shear capacity gained through the steel fibers make it attractive to use in structural members. The most of experimental and numerical studies have focused on beam members since the use of UHPFRC provides significant advantages in terms of flexural and shear behaviors. It can be also noted that balanced reinforcement ratio for the UHPFRC beam section is much greater than those of the normal and high strength fibrous concretes due to the excellent compressive strength. Thus, ductile flexural failures can be ensured even if excessive tensile reinforcements are used in the section [5,6].

Inclusion of steel fibers to the concrete mixture enhances the beam's moment capacity, stiffness and cracking behavior, but the ductility reduces due to the crack localization effect where the deformation of longitudinal reinforcement is concentrated, and the crack also widened at single point. It should be noted that this event may occur in structural member including normal and high strength fibrous concretes. Some studies point out to its negative effect on the flexural ductility for very low reinforcement ratios [6–12]. Depending on the fiber content, however, mechanical properties of the UHPFRC exhibits wide diversities so that the fiber amount and shape, fiber distribution and orientation in the concrete matrix, member dimensions can lead to differences in overall structural behavior. Numerous studies at material level were conducted to investigate effects of fiber type, amount, orientation and curing

* Corresponding author.
E-mail address: kturker@balikesir.edu.tr (K. Turker).

https://doi.org/10.1016/j.compstruct.2019.111400
Received 6 February 2019; Received in revised form 25 July 2019; Accepted 9 September 2019
Available online 10 September 2019

conditions on the flexural behavior of UHPFRC [13–21]. The current studies over the UHPFRC beams indicated that the fiber type and amount significantly affects the flexural capacity, stiffness and cracking pattern, but the flexural ductility largely depends on reinforcement ratio [6–8,22–32]. Unlike from the conventional concrete, the ductility capacity remains at low-level for low reinforcement ratios because the fibers directly change cracking behavior, but it shows an increasing trend for higher reinforcement ratios through offering pretty good compressive strength and deformation capacity. It can be drawn from the studies that the fiber content and reinforcement ratio should be compatible with each other to get the maximum flexural performance in the UHPFRC beams. Noted that researches on the structural behavior of UHPFRC beams were relatively limited for high reinforcement ratios.

Despite many investigations were conducted on the flexural behavior of UHPFRC beams, some important issues are needed to investigate both experimentally and numerically. One such issue is the hybrid fiber usage of two or more steel fiber types in the concrete mixture rather than one type. In order to improve the flexural performance of UHPFRC beams, one of the promising methods is to blend the fiber types in micro and macro forms since they differently contribute to member behavior depending upon the fiber length and diameter. In the hybrid UHPFRC mixtures, the micro fibers improve the strength and stiffness responses prior to or just after the cracking since crack widths are still small while the macro fibers limit the formation of wide (major) cracks. The micro fibers also enhance pull-out response of the fibers and thereby allow the production of members with high strength and ductile behavior [14,34–36]. In recent material-based studies regarding to impact of the hybrid fiber usage on the mechanical properties of UHPFRC, the different sized steel fibers (straight, hooked, twisted so on) were combined in the concrete mixtures [14,35–38]. It was also seen that the steel fibers were combined by non-metallic fibers in the hybrid form [39–50]. The results showed that the hybrid fiber usage leads to an increase in the energy absorption capacity and it improves the post-cracking member response in comparison to the mono fiber usage. For instance, the addition of non-metallic fibers improved the durability of UHPFRC with decreasing shrinkage or preventing spalling under elevated temperature.

Another important issue for the UHPFRC beams is related to the application of numerical design procedure in the hybrid fiber usage. The design concept for conventional concrete, where the tensile strength is ignored, cannot be directly applied to the flexural design of UHPFRC members. The member behavior with UHPFRC is more complicated than that of the conventional concrete since the compressive and post-cracking tensile behaviors majorly depend on the fiber characteristics [51]. Researches by others [6–8,29,30,52–54] and some design guidelines [55–58] proposed analytical models, in which some of them use the well-known equivalent stress block, in order to determine the moment capacity of UHPFRC beams. It can be deduced that some of these procedures gave good results under certain assumptions (i.e., member dimension, fiber content, reinforcement ratio and yield strength). However, another remarkable question arises that how to adopt the design approaches proposed for the flexural design of UHPFRC beams with the mono fiber (only short, long, single or double-hooked and twisted so on) to members containing the hybrid fibers. When the proposed numerical approaches are checked up on, the fiber contribution in tension region of strain profile is only considered for one fiber type. But there is no approach to consider the multiple fiber usage in determining the flexural capacity of UHPFRC beams.

The main purpose of this study is to investigate the flexural behavior of mono and hybrid UHPFRC beams and to develop a numerical procedure to determine the flexural moment capacity consistent with the test results. In this context, total of twelve doubly reinforced concrete beams were produced for different reinforcement ratios which represent low to excessive levels (ρ = 0.009, 0.019, 0.028 and 0.043). The first four beams consist of only short-straight fiber of 13 mm (1.5% by volume) to compare the mono and hybrid fiber usages while other quartet group includes the hybrid fiber usage where the short-straight fiber of 13 mm (1.0%) and the long-hooked fiber of 60 mm (0.5%) were blended together in the concrete mixture. Remaining group of four are the non-fiber reference beams to show the fiber contributions in the mono and hybrid forms. After conducting the four-point loading tests for all beams, the structural behaviors were discussed in terms of the load-deflection behavior, deflection and curvature ductilities, flexural stiffness, flexural moment capacity, cracking behavior and compressive strain. In the study, two numerical approaches, in which one of them uses the various fiber parameters in the matrix and other is based on the direct tensile test results, were proposed to predict the flexural capacity of UHPFRC beams in the mono and hybrid forms.

2. Experimental program

In the test program, total of twelve UHPFRC beams were produced which represent low to excessive tensile reinforcement ratios. After conducting of four-point loading tests, the parameters of load-deflection behavior, deflection and curvature ductilities, flexural stiffness, flexural moment capacity, cracking behaviors at the specific deflection values and compressive strain were discussed.

2.1. Material properties and test specimens

Three concrete mixtures were designed for the non-fiber reference beams as well as mono and hybrid UHPFRC beams. The concrete compressive strength of minimum 150 MPa and self-compacting characteristics were intended for the UHPFRC mixtures. The proportional amounts by weight of the cementitious materials, aggregates and superplasticizer are given in Table 1 for the non-fiber, mono and hybrid mixtures. However, water-to-binder ratio was kept constant as 0.18 for all mixtures. The specific material properties such as density, size and surface as well as preparation and casting procedure can be found in Hasgul et al [32]. Preparing the mono and hybrid UHPFRC mixtures, two types of steel fiber were used which are in short-straight and long-hooked forms (Fig. 1). The properties of steel fibers are listed in Table 2.

2.2. Material test specimens and setups

The compressive strengths of non-fiber and UHPFRC mixtures were obtained from uniaxial compression tests using the 100 × 100 × 100 mm^3 cube specimens. The compression tests were conducted by means of a hydraulic press under the loading rate of 1 MPa/s (Fig. 2a). However,

Table 1
Mixture proportions by weight (kg/m^3).

Mixture	C	SF	GGBS	QS1	QS2	Water	SP	Steel fiber	
								Type	Amount*
Non-fiber	690	138	276	542	542	199	17.25	—	—
Mono fiber	690	138	276	525	525	199	17.25	Short-straight	1.5%
Hybrid fiber	690	138	276	525	525	199	17.25	Short-straight	1.0%
								Long-hooked	0.5%

C: cement, SF: silica fume, GGBS: ground granulated blast-furnace slag, QS: quartz sand, SP: superplasticizer, *: Volumetric ratio.

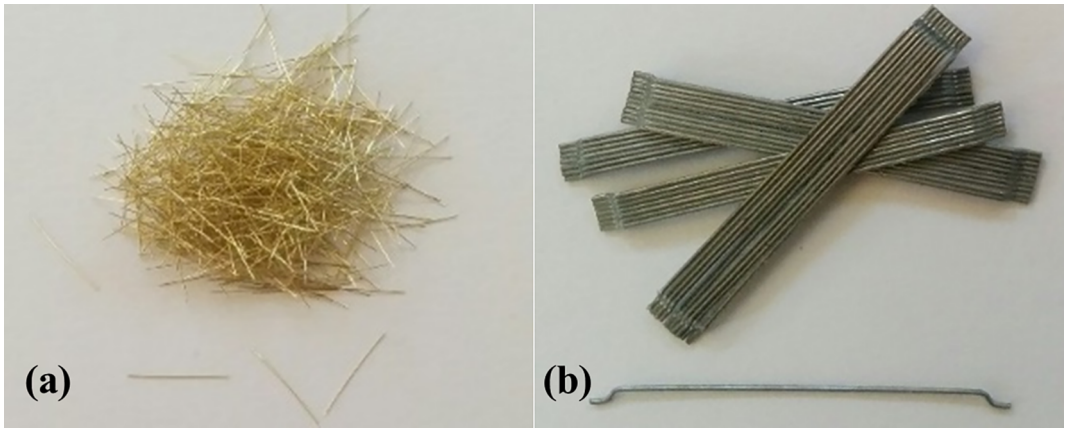

Fig. 1. Steel fibers used in the study; a) short-straight, b) long-hooked.

Table 2
Properties of steel fibers.

Type	Length (mm)	Diameter (mm)	Aspect ratio	Tensile strength (MPa)
Short-straight	13	0.16	81	2500
Long-hooked	60	0.75	80	1225

the tensile tests were conducted using the dog-bone shaped specimens (width: 68 mm, height: 240 mm, thickness: 30 mm and gauge length: 80 mm). An uniaxial load was applied to the specimen by the universal testing machine through displacement control at a rate of 0.1 mm/min (Fig. 2b). Beside these, the mechanical properties of each reinforcement group were determined by of the steel test coupons (Fig. 2c).

2.3. Test beams and structural test setup

In the study, eight UHPFRC beams and four non-fiber reference beams having four different tensile reinforcement ratios ($\rho = 0.009$, 0.019, 0.028 and 0.043) were tested. All beams were designed as doubly reinforced in order to investigate whether the UHPFRC usage can prevent the reinforcement buckling, or not. The compression reinforcements were chosen as roughly half of the tensile reinforcements. In order to guarantee the flexural failure, the stirrups with a diameter of 8 mm were provided except for the constant moment zone. This configuration removes the confinement effect of stirrups in the mid-region and also allows the investigation of buckling on the test beams. The geometric sizes and reinforcement details on a typical test beam are given in Fig. 3.

The beams were produced in three groups to study the flexural behaviors of mono and hybrid steel fibers. The first group beams of four were casted without fiber in order to show the effectiveness of the mono and hybrid fibers. While the second quartet group was produced by the mono UHPFRC mixture containing only short-straight fiber of 13 mm (1.5% by volume), the last group UHPFRC beams include the hybrid steel fibers consisting of the short-straight fiber of 13 mm (1.0%) and long-hooked fiber of 60 mm (0.5%).

The reinforcement ratios and fiber contents for the test beams are presented in Table 3. In Table 3, the notation B denotes beam and the notations NF, MF and HF point out the non-fiber, mono fiber and hybrid fiber, respectively (Table 3). Here while the beam B1 has the lowest tensile reinforcement ratio of 0.009, the beam B2 is almost correspond to the maximum reinforcement ratio in the Turkish Design Code [59]. The beams B3 and B4 represent the excessive reinforcement ratios going beyond the design codes. Thus, the wide range of reinforcement ratios could be evaluated in terms of the considered test parameters.

The static four-point loading procedure was performed for the flexural tests of beams using a servo hydraulic testing machine with maximum load capacity of 500 kN (Fig. 4). The load was divided two equal loads by a spreader beam and a distance of 700 mm between the loads. A potentiometric transducer was mounted under the mid-span of beam in order to measure vertical deflection. Determining the local curvature over the mid-span, a curvature meter setup consisting of two transducers placed on the upper and bottom sides of the beam was used as shown in

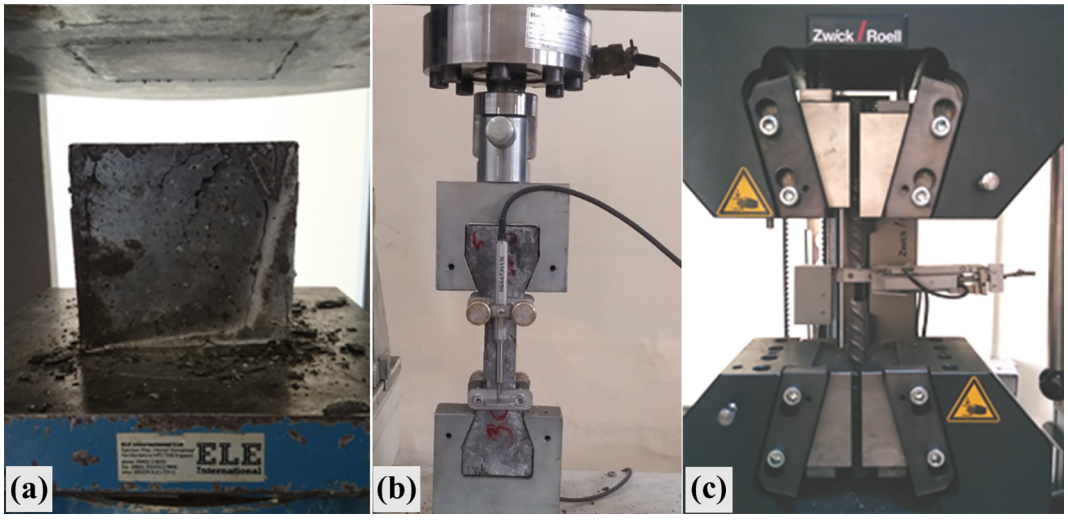

Fig. 2. Material test specimens and setups; a) uniaxial compression test setup, b) direct tensile setup, c) coupon test of reinforcement.

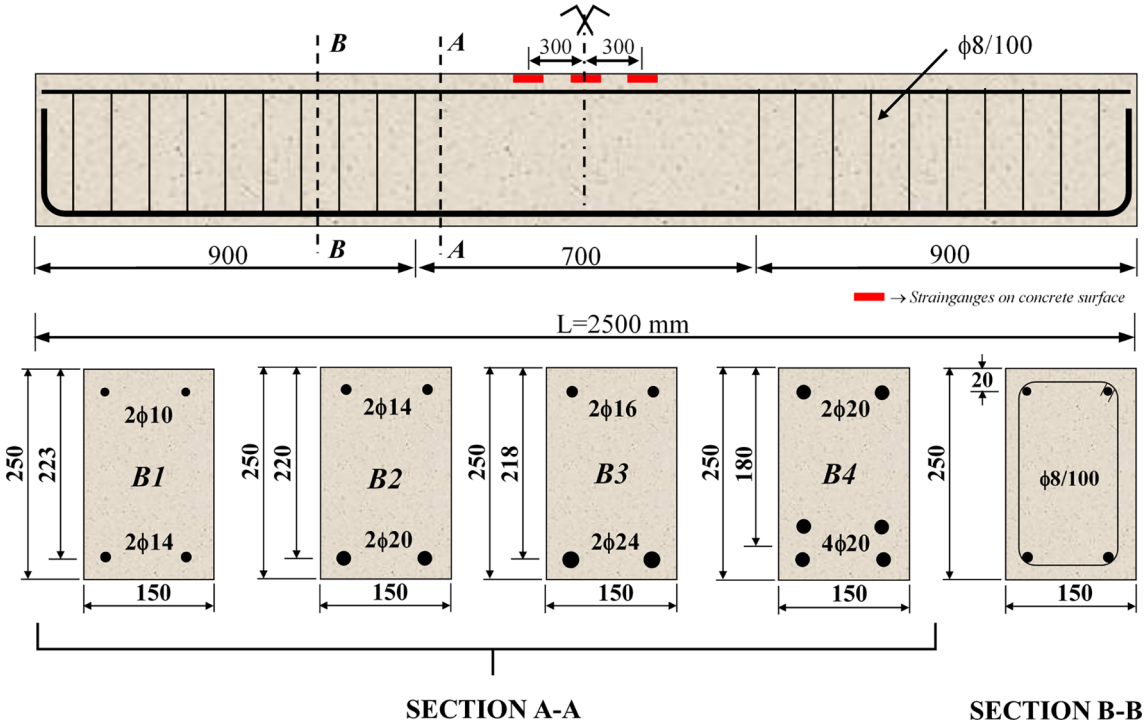

Fig. 3. Beam geometries and reinforcement details.

Table 3
Reinforcement and fiber content of test beams.

Test beam	Tensile reinforcement	Compression reinforcement	Fiber content
B1-NF	2ϕ14	2ϕ10	—
B1-MF	(ρ = 0.009)	(ρ′ = 0.005)	13/0.16 (1.5%)
B1-HF			13/0.16 (1.0%) + 60/0.75 (0.5%)
B2-NF	2ϕ20	2ϕ14	—
B2-MF	(ρ = 0.019)	(ρ′ = 0.009)	13/0.16 (1.5%)
B2-HF			13/0.16 (1.0%) + 60/0.75 (0.5%)
B3-NF	2ϕ24	2ϕ16	—
B3-MF	(ρ = 0.028)	(ρ′ = 0.012)	13/0.16 (1.5%)
B3-HF			13/0.16 (1.0%) + 60/0.75 (0.5%)
B4-NF	4ϕ20	2ϕ20	—
B4-MF	(ρ = 0.043)	(ρ′ = 0.019)	13/0.16 (1.5%)
B4-HF			13/0.16 (1.0%) + 60/0.75 (0.5%)

Fig. 4. The beams were loaded with constant displacement increments to control the mid-span deflection. Thus, the beams were loaded with a rate of 0.2 mm/s up to the peak load. Later on the displacement rate of 0.5 mm/s was used to reduce the testing time. Three strain gauges were installed to the top surface of beam to measure the compression strain of concrete (Fig. 4). The crack patterns were highlighted over the beam and the crack widths were determined with a crack width microscope.

3. Test results and discussion

3.1. Material tests

The compressive and tensile strength as well as elastic modulus of test specimens are summarized for each group in Table 4. While an average compressive strength of 145 MPa was obtained for the non-fiber beams, the compressive strengths increased 9% and 13% for the mono and hybrid fiber usages, respectively. The use of hybrid fibers did not provide a significant contribution in terms of the elastic modulus while the mono fiber increased it up to 7%. However, the average tensile strength for the non-fiber beams was determined as 4.8 MPa and this value increased to 9.32 and 11.18 MPa with the mono and hybrid UHPFRC usages, respectively. It can be noted that the hybrid fiber usage increased the tensile strength of concrete roughly 20% in comparison to the mono form (Table 4).

3.2. Structural tests

After conducting the four-point loading of all test beams, their load–deflection behaviors are given for the considered each reinforcement ratio in Fig. 5. Since all beams are under-reinforced, the ductile flexural failures were observed in the test beams, as would be expected. Noted that the steel fibers in the mono or hybrid form apparently increased the beams' initial stiffnesses and load-carrying capacities in comparison with the non-fiber versions.

As seen from the load-deflection curves presented for the mono and hybrid UHPFRC beams in Fig. 6, a deflection hardening (DH) behavior, which arise between the yield point of tensile reinforcement and peak load, was observed since the fiber use delayed the widening of flexural cracks through the fibers' bridging contribution and consequently the moment capacity increased for the beams. However, the hardening behavior ended with the fiber debonding (FD) in the tension region. The FD occurs when the load carried by one fiber exceeds the bond strength of concrete matrix. At the peak load, the fibers at a section on the beam commenced to pull out and, the strength degradations occurred after this point due to high stress in the related crack. The FD was visually observed during the tests. The FD zones are shown between the peak load and the first concrete crushing point determined by the strain gauges at the outermost compression surface of beam (Fig. 6). The fiber length and geometry are effective parameters on the FD behavior at the post-peak area where the crack width excessively enlarged due to the crack localization. It should be noted that the FD zone for the mono fiber beams decreases with increasing reinforcement ratios due to the reduced efficiency of fibers. But no specific trend could be found for the hybrid use.

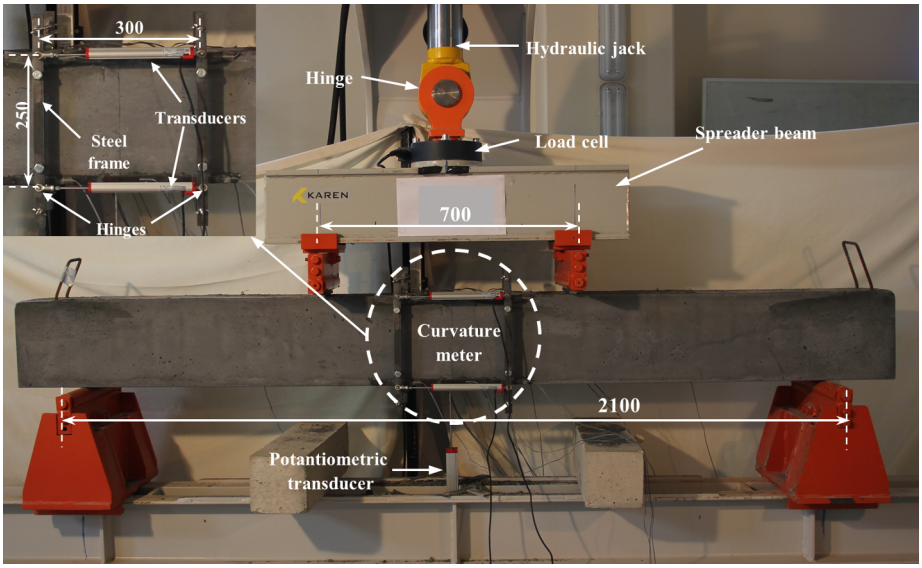

Fig. 4. Four-point bending test setup.

Table 4
The reinforcement properties and concrete strengths.

Test beam	Reinforcement						Concrete		
	Tension			Compression			Compression	Tension	Elastic modulus
	ρ	f_y (MPa)	f_u (MPa)	ρ′	f_y (MPa)	f_u (MPa)	f_c' (MPa)	σ_t (MPa)	E (GPa)
B1-NF	0.009	458	588	0.005	473	554	145	4.80	42
B1-MF		453	567		464	554	158	9.32	45
B1-HF		445	564		464	554	164	11.18	43
B2-NF	0.019	462	654	0.009	449	571	145	4.80	42
B2-MF		467	653		449	571	158	9.32	45
B2-HF		469	654		447	562	164	11.18	43
B3-NF	0.028	492	606	0.012	489	596	145	4.80	42
B3-MF		451	591		473	584	158	9.32	45
B3-HF		460	586		473	584	164	11.18	43
B4-NF	0.043	468	657	0.019	460	659	145	4.80	42
B4-MF		462	650		462	651	158	9.32	45
B4-HF		455	565		455	565	164	11.18	43

The concrete crushing (CC) failure took place along a wide region at the constant moment zone for the non-fiber beams, as shown in Fig. 7. In the non-fiber beams with low reinforcement ratios (ρ = 0.009 and 0.019), the reinforcement buckling was observed in the compression region shortly after the concrete crushing due to the lack of the confinement effect of stirrups. When further reinforcement ratios (ρ = 0.029 and 0.043) were considered, the concrete compressive block increases with going up the neutral axis depth. Thus, the stresses on compressive reinforcements reduced. On the other hand, the reduction of length to the diameter ratio of compressive reinforcement is another factor prevent the buckling. However, for the UHPFRC beams, regardless of the mono or hybrid fiber usage, the deformation of tensile reinforcement concentrated at the point where one major crack was widened on the beam. This crack width intensely enlarged as against other cracks as shown in Fig. 7. Despite the concrete crushing occurred in the case of UHPFRC beams, the concrete cover remained intact through the confinement effect of fibers and they did not allow buckling of the compressive reinforcement. All the UHPFRC beams failed as a result of the tensile reinforcement rupture (RR) for all reinforcement ratios.

3.2.1. Deflection and curvature ductility

The ductility values of non-fiber and UHPFRC beams were compared to each other to show the flexural performance of mono and hybrid fiber usages. The deflection ductility (μ_Δ) is determined by proportioning the ultimate deflection (Δ_u) to yield deflection (Δ_y). The yield deflection was obtained from the bi-linearized load-deflection behavior, which is one of the methods recommended in Park [60]. This deflection point corresponds to the displacement at the intersection of the secant stiffness at 75% of the peak load (P_p) with the peak load level (Fig. 8).

All UHPFRC beams maintained their stability pretty good even at the deflections up to strength decreasing of 20% after the peak load. After this point, some stability problems might occur on the beams. It should be noted that the non-fiber beams have no deflection capacity after the peak load due to the concrete crushing. On the other hand, Park [60] proposed some procedures to specify the ultimate deflection (Δ_u) of experimental load-deflection behavior. One of these procedures, which is known as 20% load reduction method and is widely used to determine the ultimate deflection point, was based on in the study. The deflection ductilities and other characteristic values for the mono and hybrid UHPFRC beams are presented in Fig. 9a and Table 5. Moreover, the ductilities calculated for the UHPFRC beams were proportioned to those of the non-fiber beams to see effectiveness of different fiber usages (Fig. 9b).

For the non-fiber beams, the deflection ductility decreased from 8.14 to 2.11 with increasing of the tensile reinforcement ratio, as expected (Table 5 and Fig. 9a). For the UHPFRC beams in the mono form, where only 13 mm straight-fiber is used, although the deflection ductility for

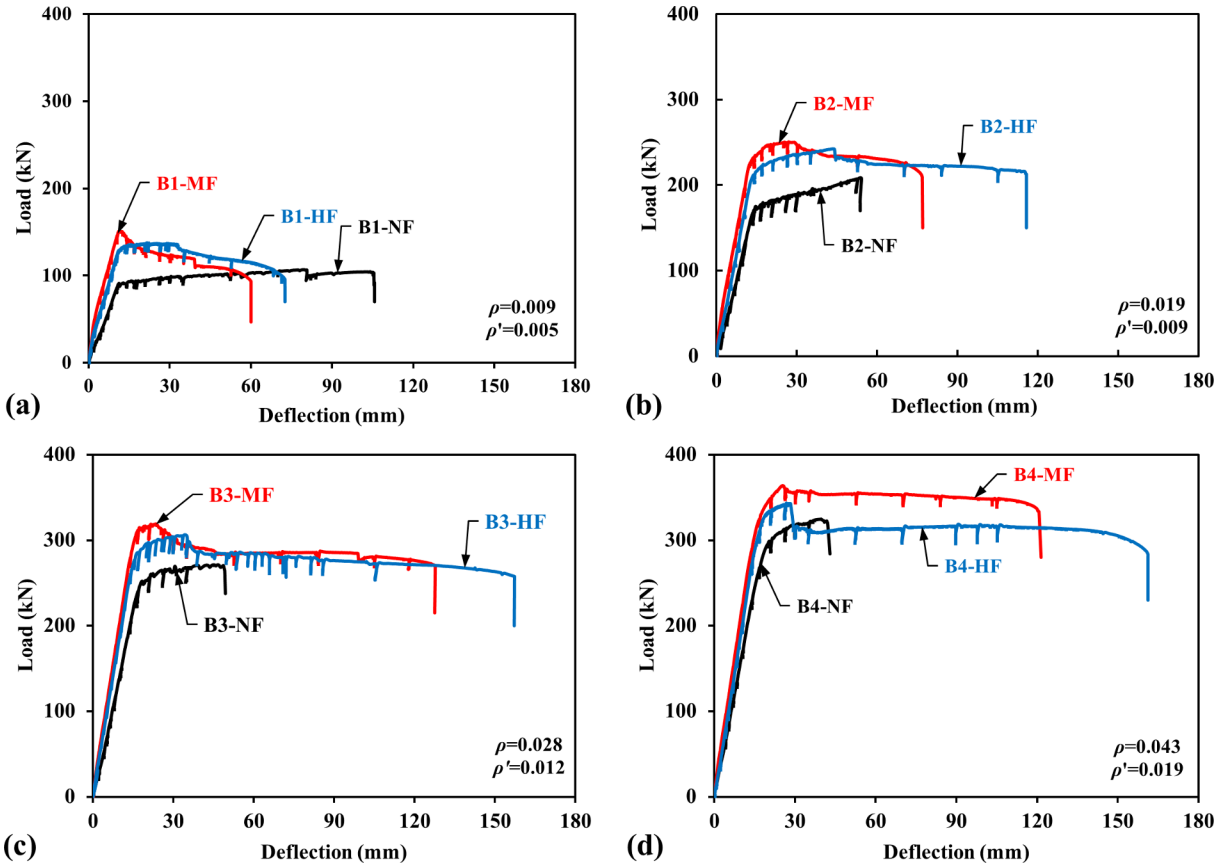

Fig. 5. Load–deflection relationships; a) ρ = 0.009, b) ρ = 0.019, c) ρ = 0.028, d) ρ = 0.043.

the lowest reinforcement ratio of 0.009 decreased 2.3 times in comparison with the non-fiber beam, the ductility values and fiber effectiveness significantly increased as the reinforcement ratio increases. In a similar manner, the ductilities for the hybrid beams showed an increasing trend with the reinforcement ratio. For the non-fiber test beams, the flexural cracks in the constant moment zone widened almost uniform as in the conventional normal or high strength reinforced concrete. It was observed that these beams failed by concrete crushing at the compression zone after the reinforcement yielding. Thus, the concrete crushing occurred at lower deflection values due to the increased reinforcement ratio. Hence, the deflection ductility showed a decreasing trend, as would be expected. Despite that, the deformation of longitudinal reinforcement for the UHPFRC beams was concentrated at the point where a single crack widened due to the crack localization. Later on, the reinforcement rupture occurred prematurely prior to the concrete failure. It was also noted that the rupture failure occurred at higher deflections, despite the crack localization, with the increase of reinforcement ratios through the excellent deformation capacity of UHPFRC under compression. Consequently, the ductility increased for the UHPFRC beams.

It can be noted that the ductility values of hybrid beams are greater than those of the mono beams for each reinforcement ratio. However, even when the excessive reinforcement ratios were used in the mono and hybrid fiber beams, the ductility values increased 3.33 and 4.35 times in comparison with the non-fiber beams, respectively (Fig. 9b). The highest ductility among the test beams was achieved for the beams B3-MF and B3-HF having the reinforcement ratio of 0.028. This ratio is well above the limits in many design codes. It can be deduced that higher reinforcement ratios can be used to benefit from the UHPFRC's excellent compressive and deformation capacities. The hybrid fiber usage in the UHPFRC beams gives better performance in terms of the deflection ductility.

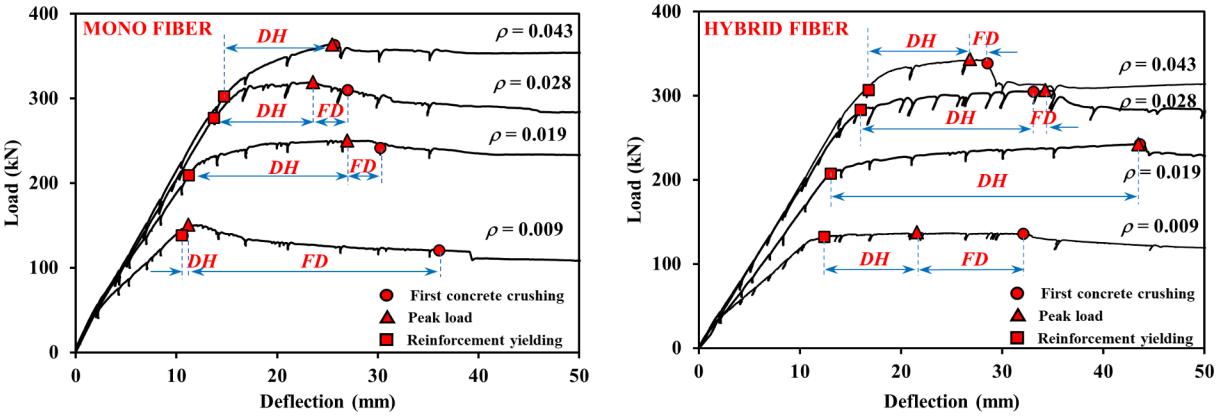

Fig. 6. Deflection hardening and fiber debonding responses of UHPFRC beams.

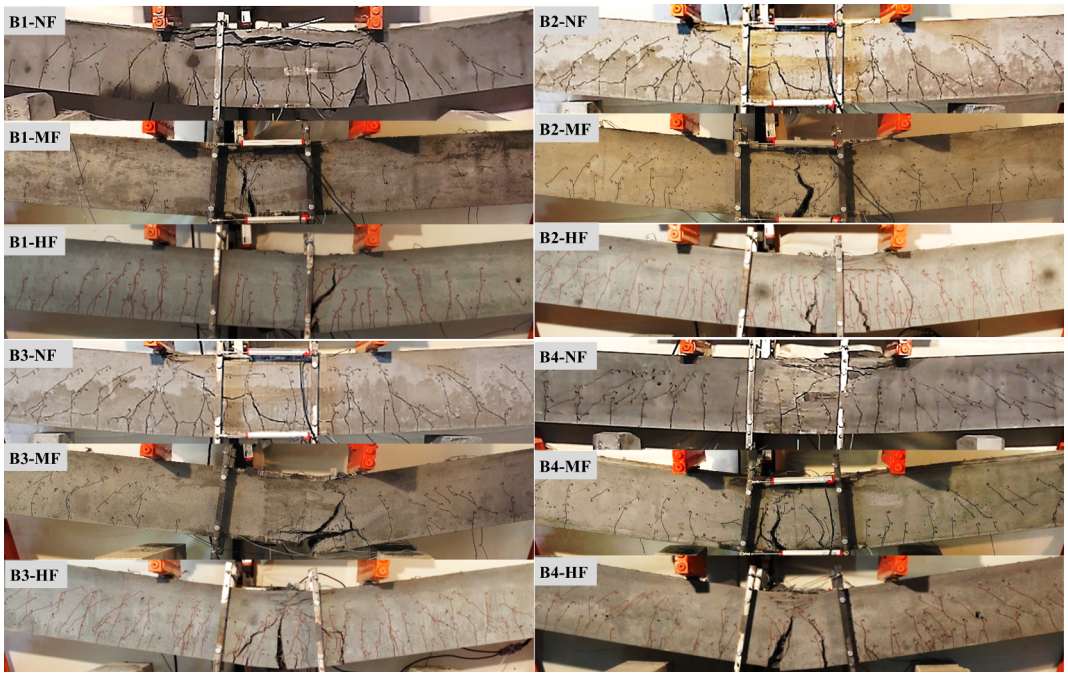

Fig. 7. Failure patterns of the non-fiber and UHPFRC beams.

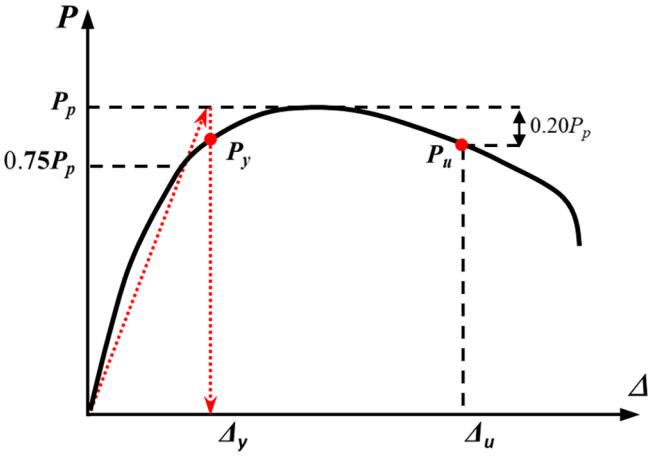

Fig. 8. Bi-linear idealization of load-deflection behavior [60].

In the test program, the moment-curvature relationships were also determined from the measurements at the constant moment zone of beams. The moment-curvature curve for the beam B4-NF early terminated because of the damage caused by the crushing on the beam's top surface. Moreover, because the major crack on the beam B1-HF developed out of the curvature-meter, the measurement could not be completed after the peak load (Fig. 10).

The curvature ductility (μ_ϕ) and flexural stiffness (EI_{eff}) of the UHPFRC beams were determined by the moment–curvature curves for the considered each reinforcement ratio. The curvature ductilities (μ_ϕ) were determined by proportioning the ultimate curvature (ϕ_u) to yield curvature (ϕ_y). The idealization procedure used in calculation of the deflection ductility was considered again for these characteristic values. The curvature ductilities and other characteristics values are presented in Table 6. The variation of ductilities with the reinforcement ratios are also given in Fig. 11a.

As shown from the Fig. 11a and Table 6, the curvature ductilities for the non-fiber beams decreased from 8.26 to 4.67 for the increasing reinforcement ratios. Due to the crack localization behavior, overly high curvature ductilities were obtained for the UHPFRC beams. The curvature ductilities for the mono and hybrid beams showed a variation in a range of 11.07 to 25.06 and 14.98 to 33.11, respectively.

Despite the curvature ductility for the mono fiber beam (B3-MF) with ρ = 0.028 somewhat decreased, the ratios gained an increasing tendency with the mono and hybrid fiber usages (Fig. 11a). The

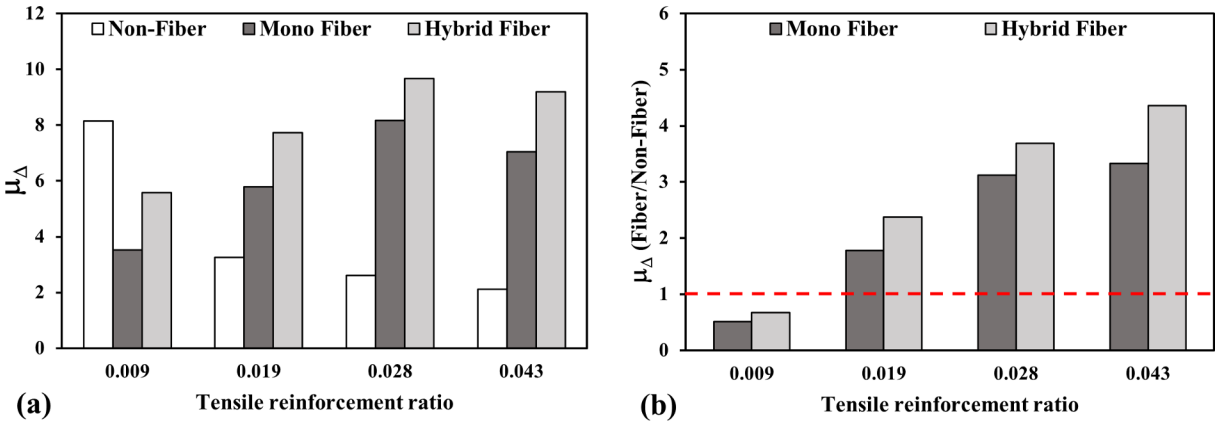

Fig. 9. a) Variation of deflection ductilities, b) Effectiveness of steel fibers on ductility.

Table 5
Characteristic values for the load–deflection behavior.

Test beam	Δ_y (mm)	P_y (kN)	Δ_p (mm)	P_p (kN)	Δ_u (mm)	P_u (kN)	μ_Δ	Failure mode
B1-NF	12.96	91.25	79.27	106.80	105.49	102.31	8.14	CC
B1-MF	10.22	142.63	11.19	150.78	36.13	120.69	3.54	RR
B1-HF	11.78	128.76	21.56	137.58	65.64	110.66	5.57	RR
B2-NF	16.66	177.06	53.74	208.65	54.15	206.14	3.25	CC
B2-MF	13.28	229.62	26.97	250.58	76.83	208.99	5.79	RR
B2-HF	14.98	216.23	43.49	242.33	115.76	212.23	7.73	RR
B3-NF	18.57	249.98	46.51	271.39	48.68	270.31	2.62	CC
B3-MF	15.63	302.23	23.55	319.16	127.70	266.92	8.17	RR
B3-HF	16.28	284.52	35.99	306.37	157.25	257.71	9.66	RR
B4-NF	19.89	295.21	39.70	324.81	42.00	320.93	2.11	CC
B4-MF	17.16	328.62	25.46	363.93	120.70	333.48	7.03	RR
B4-HF	17.54	319.14	26.81	343.38	161.18	284.06	9.19	RR

P_y: yield load, P_p: peak load, P_u: ultimate load, Δ_y: yield deflection, Δ_p: deflection of the peak load, Δ_u: ultimate deflection, μ_Δ: deflection ductility, CC: concrete crushing, RR: reinforcement rupture.

maximum curvature ductilities were obtained for the beams B4-MF and B4-HF including the highest reinforcement ratio (ρ = 0.043). It can be also noted that the hybrid beams showed better performance in comparison with the mono usage as in the deflection ductility.

However, the effective flexural stiffness (EI_{eff}), which is the ratio of the peak moment (M_p) to the yield curvature (ϕ_y) on the idealized elasto-plastic response, was calculated by using ascending branch of the moment-curvature curves (Table 6 and Fig. 11b). While a significant stiffness increase was determined for the mono and hybrid UHPFRC beams with the lowest reinforcement ratio, this change remained limited for the further ratios. It can be also noted that the flexural stiffnesses obtained from the mono fiber beams were slightly more than the hybrid form (Fig. 11b).

3.2.2. Flexural moment capacity

In order to determine the effectiveness of steel fiber to the flexural moment capacities of beams produced in the mono or hybrid form, the moment capacities (M_p) were proportioned to those obtained from the non-fiber beams. The increases of 6–41% in the moment capacities were obtained through the different contribution of fibers compared to the non-fiber beams. The greatest increase was obtained for the beam B4-MF having the mono fiber and the highest reinforcement ratio. However, the moment capacities of the hybrid beams are slightly smaller than the mono beams since the volumetric ratio of short fiber in the hybrid mixture is less and it governs the strength and stiffness responses prior to the cracking. It can be also noted that as the tensile reinforcement ratio increases, the fiber contribution on the moment capacity decreased for both fiber usages as shown in Fig. 12.

3.2.3. Cracking behavior

The cracking patterns and crack widths of the mono and hybrid fiber beams were compared to the non-fiber versions to show the effectiveness of fibers on the cracking behavior. The cracking behaviors

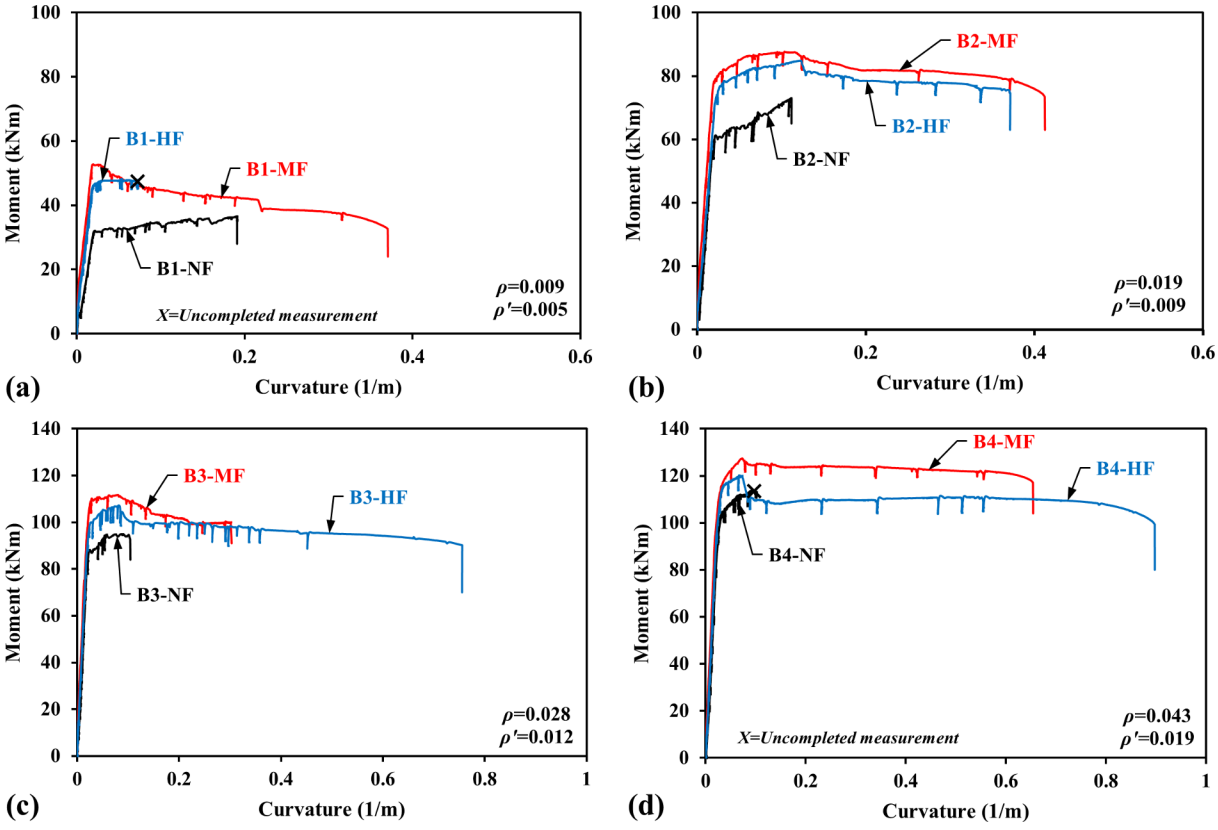

Fig. 10. Moment–curvature relationships; a) ρ = 0.009, b) ρ = 0.019, c) ρ = 0.028, d) ρ = 0.043.

Table 6
Characteristic values for moment-curvature behavior.

Test beam	ϕ_y (1/m)	M_y (kNm)	ϕ_p (1/m)	M_p (kNm)	ϕ_u (1/m)	M_u (kNm)	μ_ϕ	EI_{eff} (kNm^2)
B1-NF	0.0231	31.73	0.1909	37.38	0.1909	35.53	8.26	1618
B1-MF	0.0178	50.11	0.0191	52.77	0.1971	42.17	11.07	2963
B1-HF	0.0184	45.26	0.0525	48.15	xxx	xxx	xxx	2617
B2-NF	0.0227	60.98	0.1112	73.03	0.1117	72.15	4.92	3217
B2-MF	0.0207	78.51	0.1035	87.70	0.4122	73.38	19.91	4237
B2-HF	0.0248	75.41	0.1217	84.82	0.3715	74.47	14.98	3420
B3-NF	0.0223	86.42	0.0898	94.99	0.1041	92.72	4.67	4259
B3-MF	0.0216	101.13	0.0803	111.71	0.3013	99.98	13.95	5172
B3-HF	0.0230	96.16	0.0814	107.23	0.7555	90.20	32.85	4662
B4-NF	0.0269	99.04	0.0956	113.68	xxx	xxx	xxx	4226
B4-MF	0.0261	110.06	0.0727	127.38	0.6540	116.95	25.06	4880
B4-HF	0.0271	106.44	0.0664	120.18	0.8974	99.32	33.11	4435

M_y: yield moment, M_p: peak moment, M_u: ultimate moment, ϕ_y: equivalent yield curvature, ϕ_p: curvature of the peak moment, ϕ_u: ultimate curvature, μ_ϕ:curvature ductility, EI_{eff}: effective flexural stiffness.

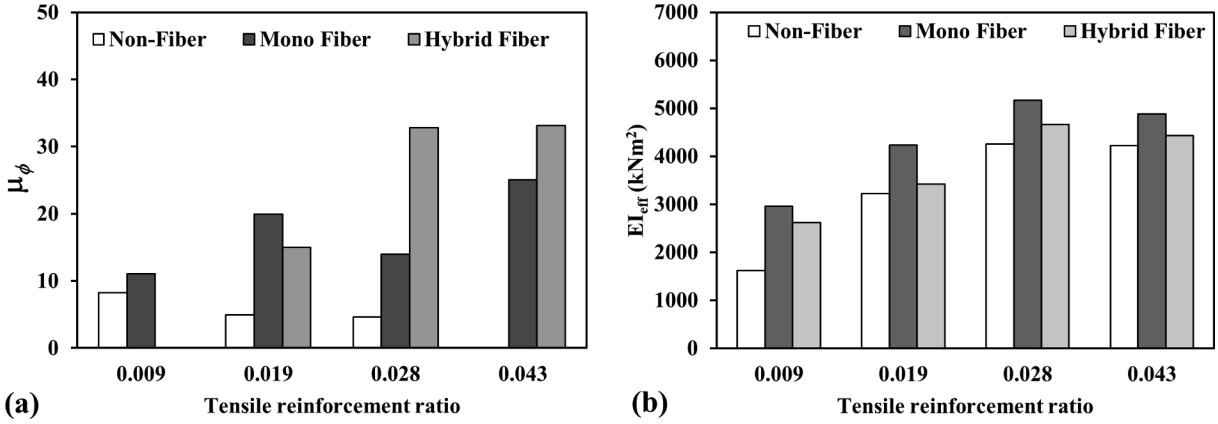

Fig. 11. a) Variation of curvature ductilities, b) Variation of effective flexural stiffnesses.

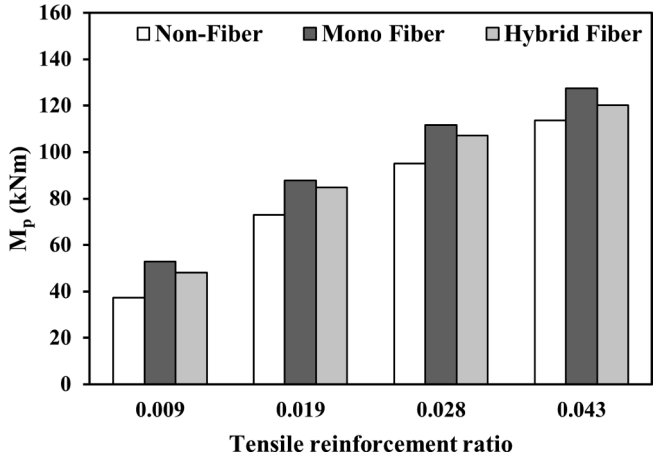

Fig. 12. Flexural capacities of the test beams.

were investigated at the specific deflections of $L/250$ and $L/70$. While the value $L/250$ corresponds to the serviceability limit state (SLS) in elastic region, the value $L/70$ represents the ultimate limit state (ULS) representing significant inelastic deformations [32]. The crack widths and cracking patterns for both limit states are shown in Figs. 13, 14 and 15, respectively.

It was observed for the SLS that the total number of cracks in the mono fiber beams significantly decreased and this fiber usage limited the crack widths ranged from 20% to 58% in comparison with the non-fiber beams. However, the hybrid fiber beams could not show good performance comparing to others for this limit state (Figs. 13 and 14). The main reason is that the amount of micro fiber in the mixture (1.0% by volume) is not sufficient to limit the crack widths and the long fibers are not already activated. The authors think that if more short fiber in the hybrid mixture would be considered, better cracking behavior could be achieved for this limit state.

For the ULS after the peak load, the maximum crack widths for the mono fiber beams considerably increased range from 3.8 to 6.8 times. While the straight fibers were not able to restrict the formation of major crack due to their short length, the hybrid fiber usage significantly limited to the crack widths for the reinforcement ratios of 0.019 and above since the long-hooked fibers effectively bridged the major cracks and the most of short-straight fibers already pulled out. Consequently, while the combined use of short and long fibers is effective for both limit states, the mono fiber usage can be effective for only one depending on the length of fibers.

3.2.4. Concrete strain response

The compressive strain response of concrete is important for the flexural design of reinforced concrete members. However, the UHPFRC exhibits more ductile behavior under compression by means of contribution of steel fibers and it has a large deformation capacity after the peak. It should be noted that the design limits corresponding to the normal strength concrete are not compatible with both high strength fiber reinforced concrete and UHPFRC. Hereat, the compressive strain limit should be investigated taking into account the fiber parameters. Therefore, the concrete strains were measured at the outermost compression surfaces of the beam mid-region (Fig. 16a-b). As shown from the load-strain behaviors, the strain values continue to increase until the first concrete crushing. Later on, the values measured by the strain gauges begin to decrease because the stresses in compression region decrease. It was observed that the characteristic responses of

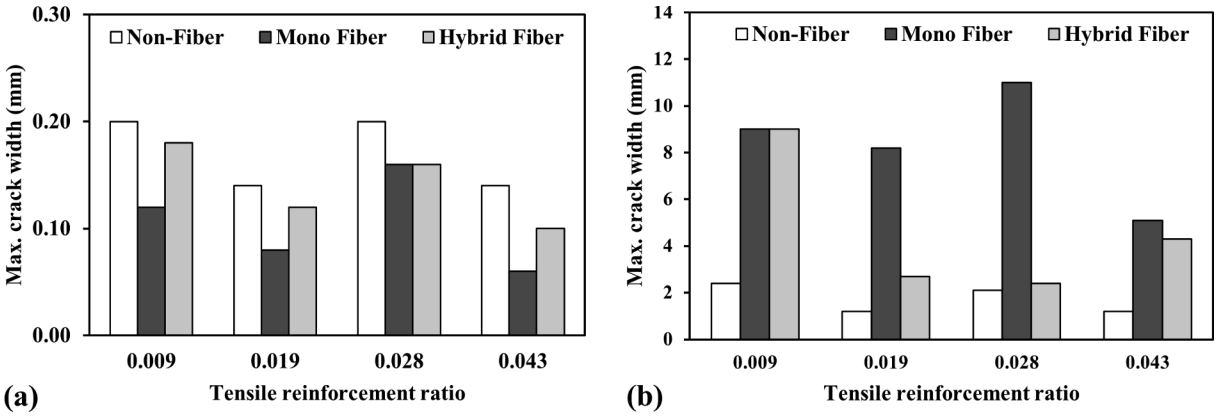

Fig. 13. Maximum crack widths; a) *L*/250, b) *L*/70.

compressive strains are regardless of the reinforcement ratio and fiber usage. While an average concrete strain of 0.0033 was obtained for the non-fiber beams, this value was nearly 0.004 for the mono and hybrid UHPFRC beams. This result is quite consistent with the strain limits suggested in the ACI 544 [61].

4. Numerical calculation of flexural moment capacity

In the current design codes, the design principles developed for the conventional reinforced concrete structures have been introduced and used in practice successfully. However, these principles cannot be directly applied to the flexural design of UHPFRC members since the compressive, tensile and strain-hardening behaviors of the concrete are distinct from the conventional concrete. Although some recommendations [55–58] were presented with regard to flexural moment capacity of members with the UHPFRC, these approaches have not been included yet in a design standard and code such as ACI, IBC and Eurocode. However, numerous models were proposed to describe the nonlinear behavior of UHPFRC [6–8,25,28,51,54]. These studies are principally based on moment-curvature analysis and they require the use of stress-strain relationships in the compression/tension as well as additional material tests which are difficult to apply for the design purpose. Thus, developing of the design oriented-simplified methods became important to predict the moment capacities of beams. Many efforts were made for the members with both high strength and ultra-high strength fiber reinforced concrete investigating the shape of concrete stress block, ultimate strain capacity, fibers' geometrical properties (such as, material, type, aspect ratio), volumetric ratio, orientation, bond stress as well as other parameters affecting the tensile stress distribution [12,24–26,52–54,62,63]. It should be noted that these studies just focused on the mono fiber usage and no numerical approach or recommendation has been presented for the hybrid fiber usage where two or more fiber types are blended together in the concrete mixture.

In this study, two numerical approaches were proposed to predict the nominal moment capacity of UHPFRC beams produced in the mono or hybrid form. Both approaches are essentially same, but the calculation procedures for the tensile strength of UHPFRC are different. The analysis procedure is based on the model proposed for the normal strength fibrous concrete beams in ACI 544 [61]. Here the use of equivalent stress block was maintained for the compression and tension regions. However, some improvements were made on the existing model in order to be compatible with the test results. For example, although the strain limit at the outermost compression surface was given 0.003, it was noted that the strain value 0.004 can be taken for the members containing the fibers of 1.0–3.0% by volume. Thus, the proposed approach assumes this limit value. This assumption is quite consistent with the experimental strain behaviors of the mono and hybrid UHPFRC beams in this study (Fig. 16).

In the proposed first approach, the tensile strength of concrete is calculated by considering some fiber parameters (such as, fiber type, aspect ratio, orientation and volumetric ratio so on) and bond strength between the fiber and concrete matrix. The second approach uses final tensile strength obtained from direct tensile test in order to eliminate uncertainties in determining the fiber parameters. The parameters related to the tensile strength of UHPFRC were optimized to ensure that both approaches are compatible with each other as well as the experimental results. Both approaches were applied to the UHPFRC test beams and the results were compared to the test results. In addition, in

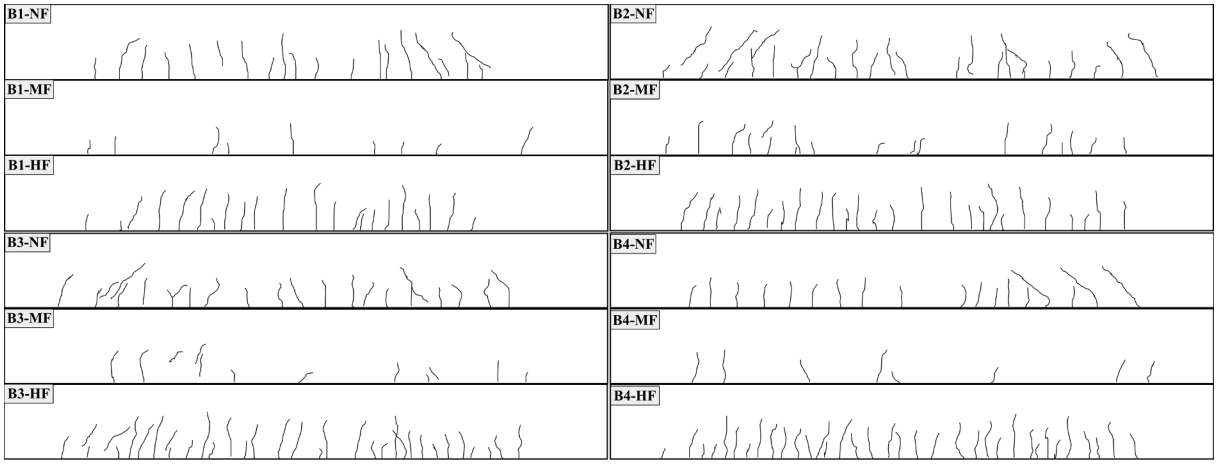

Fig. 14. Cracking patterns at the *L*/250.

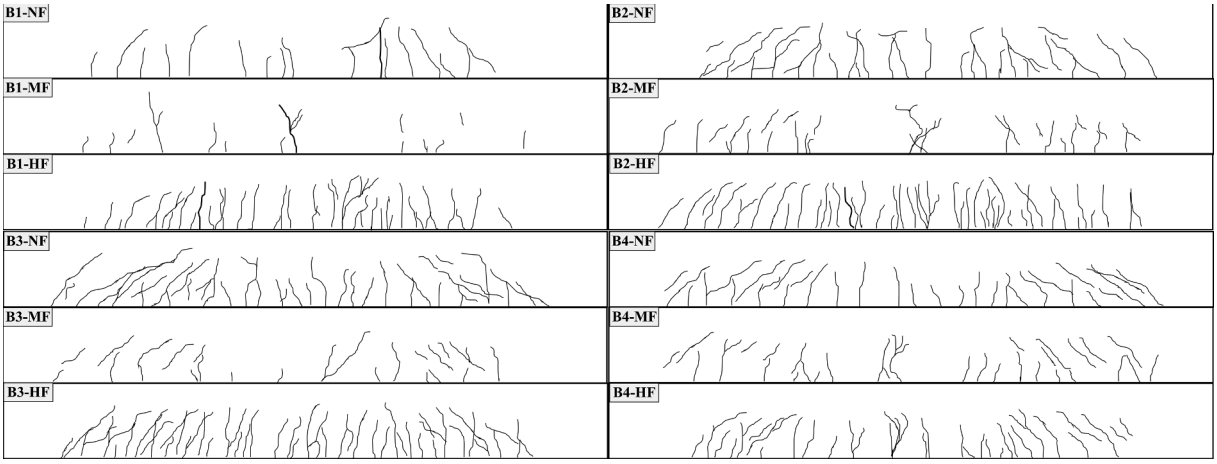

Fig. 15. Cracking patterns at the *L*/70.

order to investigate applicability of these approaches in member design, they were applied to various UHPFRC beams previously studied in literature.

Approach 1: The ACI 544 [61] procedure is commonly used in many studies [12,52,53,62,63] for predicting the nominal moment capacity of singly reinforced fibrous concrete beams. This model uses the equivalent stress block at the compression and tension regions of concrete as shown in Fig. 17. The tensile strength (σ_t) is calculated by Eq. (1). Assumed that the yield condition of tensile reinforcement governs the ultimate capacity.

$$\sigma_t = 0.00772\left(\frac{l_f}{d_f}\right)\rho_f F_{be} \tag{1}$$

Here, l and d_f denote the fiber length and diameter, ρ_f is the volumetric fiber ratio and F_{be} is the bond efficiency of fibers.

The Eq. (1) proposed for the tensile strength (σ_t) is based on fiber-matrix bond strength (τ_f) of 2.3 MPa for the normal strength concrete [61]. For the high strength fibrous concretes, this value should be greater than that of the normal strength concrete due to their dense matrix. Naaman and Najm [64] stated that the bond strength value is in a range of 1–9 depending upon the concrete compressive strength and fiber characteristics. For high strength concrete, Imam et al. [53] used the bond strength value of 4.15 MPa recommended by Al-Ta'an and Al-Feel [65]. Accordingly, the coefficient 0.00772 in the Eq. (1) was modified as 0.02 and the tensile strength expression was transformed to Eq. (2).

$$\sigma_t = 0.02\left(\frac{l_f}{d_f}\right)\rho_f F_{be} \tag{2}$$

Khalil and Tayfur [52] modified the Eq. (1) in the form of Eq. (3) for the UHPFRC beams. The bond strength parameter (τ_f) in Eq. (3) is 7.7 MPa for the average compressive strength of 136 MPa.

$$\sigma_t = 0.85\rho_f \tau_f \left(\frac{l_f}{d_f}\right) \tag{3}$$

In the current study, a parametrical study was conducted in accordance with the test results of UHPFRC beams, and consequently the bond strength value was optimized to 8.15 MPa for the mono and hybrid beams. In the approach 1, the tensile strength of UHPFRC (σ_{t1}) is calculated by Eq. (4) which is firstly proposed by Ahmed and Pama [66] and later modified by Kahlil and Tayfur [52]. This equation considers various fiber characteristics such as fiber orientation, adherence, length, amount, aspect ratio and bond strength. In accordance with the ACI 544, the tensile stress block begins a distance of e from the outermost compression surface (Fig. 17) and the length e can be calculated by Eq. (5).

$$\sigma_{t1} = 2\eta_o \eta_b \eta_l V_f \tau_f \left(\frac{l_f}{d_f}\right) \tag{4}$$

$$e = [\varepsilon_s(fibers) + 0.004] * \frac{c}{0.004} \tag{5}$$

In the Eq. (4), efficiency factors η_o and η_l representing the fiber orientation and length in the concrete matrix are taken as 0.86 and 0.41, respectively [67,68]. The bond efficiency factor (η_b) is 1.0 and 1.2 for the straight and hooked fibers, respectively [61]. It can be noted that these factors are regardless of the normal strength or high strength concrete usage and they mostly depend on the fiber characteristics in the matrix.

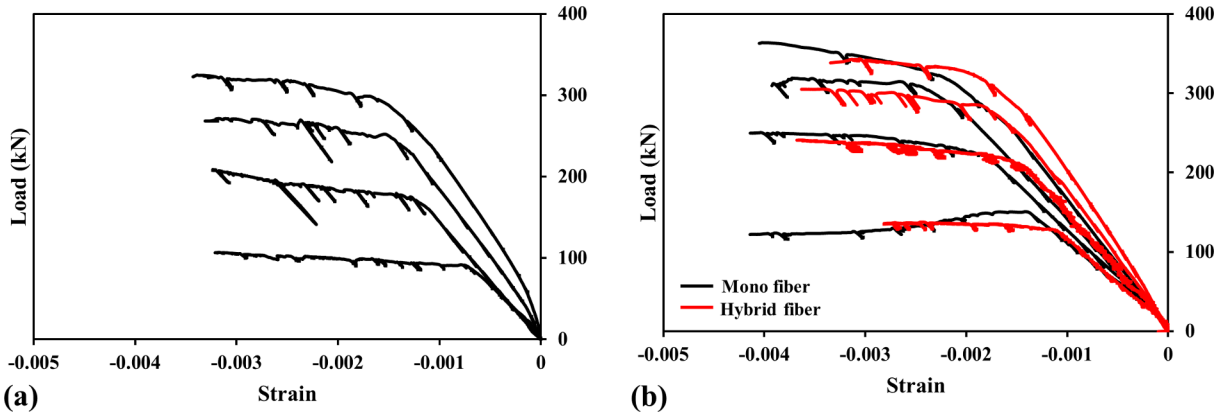

Fig. 16. Compressive strains behaviors of the beams; a) Non-fiber, b) UHPFRC.

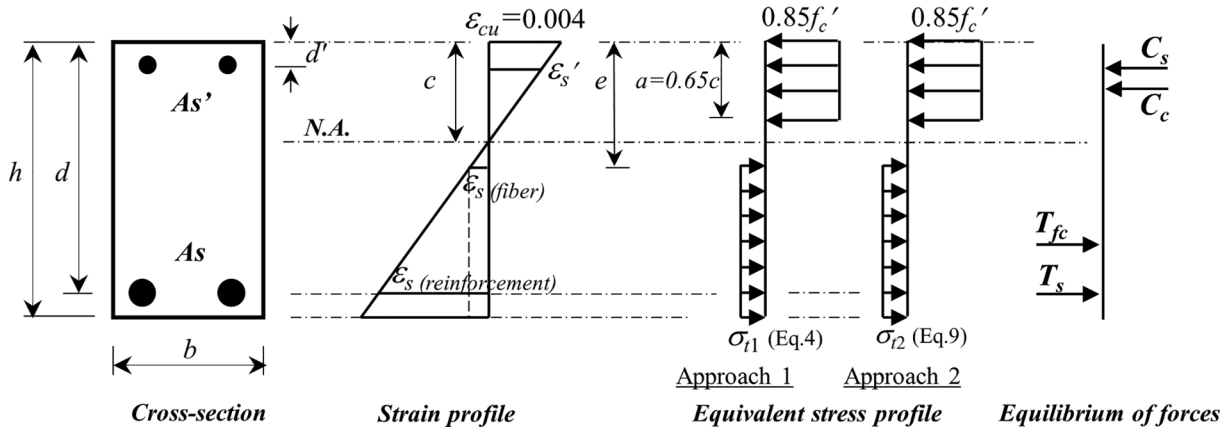

Fig. 17. Strain and stress distributions for proposed approaches.

When the numerical models are checked up on for the normal, high and ultra-high strength reinforced concretes, the fiber contribution in strain profile is considered for only single fiber type. Hence, there is no answer to the question of how to adopt the current tensile strength equations developed for the mono fiber concrete to the hybrid UHPFRC. Therefore, an approach was conducted to calculate the parameters which depends on fiber length in tensile strength of the hybrid concrete. In this context, the fiber length, diameter and bond efficiency factor were determined by proportioning the volumetric ratio of each fiber type in the mixture to the total fiber ratio (Eqs. (6)–(8)). For instance, the related parameters for a hybrid mixture containing the short-straight fiber 13/0.16 (1.0%) and long-hooked fiber 60/0.75 (0.5%) can be calculated as; $l_f = 13x(1.0/1.5) + 60x(0.5/1.5) = 28.67$ mm, $d_f = 0.16x(1.0/1.5) + 0.75x(0.5/1.5) = 0.36$ mm, $\eta_b = 1.0x(1.0/1.5) + 1.2x(0.5/1.5) = 1.07$

$$l_f = l_{f1}\left(\frac{V_{f1}}{V_f}\right) + l_{f2}\left(\frac{V_{f2}}{V_f}\right) + \cdots + l_{fn}\left(\frac{V_{fn}}{V_f}\right) \quad (6)$$

$$d_f = d_{f1}\left(\frac{V_{f1}}{V_f}\right) + d_{f2}\left(\frac{V_{f2}}{V_f}\right) + \cdots + d_{fn}\left(\frac{V_{fn}}{V_f}\right) \quad (7)$$

$$\eta_b = \eta_{b1}\left(\frac{V_{f1}}{V_f}\right) + \eta_{b2}\left(\frac{V_{f2}}{V_f}\right) + \cdots + \eta_{bn}\left(\frac{V_{fn}}{V_f}\right) \quad (8)$$

Here l_{f1}, l_{f2},…,l_{fn}; d_{b1}, d_{b2},…,d_{bn}; η_{b1}, η_{b2},…, η_{bn} and V_{f1}, V_{f2},…, V_{fn} denote, respectively, the fiber length, fiber diameter, bond efficiency factor and volumetric ratio for each fiber type.

Approach 2: The second proposed approach is essentially same with the approach 1, but it uses direct tensile test results in order to eliminate possible uncertainties in the fiber parameters specified in Eq. (4). The use of equivalent stress block for the compression and tension regions as well as the stress and strain profiles are still maintained. However, the tensile strengths ($\sigma_{t,\exp}$) must be reduced by a coefficient to get equivalent tensile block as in the compression block (Fig. 17) [26]. In this context, the strength reduction factor (k) was parametrically investigated on the test beams and was optimized to 0.75 as shown in Eq. (9).

$$\sigma_{t2} = k * \sigma_{t,exp} \quad (9)$$

The calculation procedures for the specified two approaches were coded through the *Matlab* platform to determine the flexural moment capacities of UHPFRC beams in the mono or hybrid form. So firstly, the tensile strength of UHPFRC is calculated by Eqs. (4) or (9). Then, the neutral axis depth (c) is determined by controlling the equilibrium of forces in the compression and tensile regions depending on the strain and the stress profiles in the Fig. 17. Finally, the moment capacity of beam is calculated by taking a moment of forces about the neutral axis location.

Both approaches were applied to the doubly reinforced UHPFRC test beams, and the calculated moment capacities ($M_{p,cal}$) were proportioned to the experimental capacities ($M_{p,\exp}$) to show how the proposed methods give results. The comparison results and statistical evaluation parameters, such as mean, standard deviation (*Std*) and coefficient of variation (*CoV*) for $M_{p,cal}/M_{p,\exp}$ values, are given in Table 7.

As shown in Table 7, both procedures are highly compatible with each other even though one of them uses the fiber parameters in the UHPFRC matrix and other uses the direct tensile test results. However, the numerical capacities calculated for the mono and hybrid UHPFRC beams are in good agreement with the test results for the reinforcement ratios of 1.9% and above, but they overestimate the capacities for the lowest reinforcement ratio, as would be expected. Nevertheless, it can be deduced that both approaches can determine the flexural moment capacities of UHPFRC beams in a band of 10%.

The proposed approaches were also applied to UHPFRC beams previously tested in research by others [6,8,26,32,33] to see applicability of them in member design. The cross-sectional dimensions, longitudinal reinforcement details and mechanical properties, fiber contents, concrete and tensile strengths used in these studies are summarized in Table 8. The total of 24 singly reinforced test beams were analyzed using the approaches 1 and 2, and the numerical results were compared to the test results in Fig. 18a-b and Table 8.

It is evident from these results that the proposed approaches can determine the moment capacities of UHPFRC beams within a band of ± 15% even though the dimensions, reinforcement ratios, yield strengths compressive/tensile behaviors are quite different as well as they were produced probable different casting techniques.

5. Conclusions

In this study, the flexural behavior of Ultra-High Performance Fiber

Table 7
Summary of numerical analyses for the mono and hybrid UHPFRC beams.

Test beam	$M_{p,\exp}$ (kNm)	Approach 1		Approach 2	
		$M_{p,cal}$ (kNm)	$\frac{M_{p,cal}}{M_{p,\exp}}$	$M_{p,cal}$ (kNm)	$\frac{M_{p,cal}}{M_{p,\exp}}$
B1-MF	52.77	61.58	1.17	61.57	1.17
B2-MF	87.70	90.60	1.03	90.56	1.03
B3-MF	111.71	110.94	0.99	110.93	0.99
B4-MF	127.38	130.43	1.02	130.42	1.02
B1-HF	48.15	62.82	1.30	66.45	1.38
B2-HF	84.82	92.62	1.09	96.08	1.13
B3-HF	107.23	114.24	1.07	117.61	1.10
B4-HF	120.18	130.92	1.09	134.18	1.12
Mean			1.10		1.12
Std			0.10		0.12
CoV			0.09		0.11

Table 8
Summary of beam properties and calculated/experimental moment capacities.

Test beam	b (mm)	h (mm)	d (mm)	A_s (mm^2)	f_y (MPa)	l_f/d_f (mm)	ρ_f (%)	$M_{p,exp}$ (kNm)	Approach 1		Approach 2	
									$M_{p,cal}$ (kNm)	$\frac{M_{p,cal}}{M_{p,exp}}$	$M_{p,cal}$ (kNm)	$\frac{M_{p,cal}}{M_{p,exp}}$
Yang et al. (2010), f_c' = 194 MPa, σ_t = 11.6 MPa												
R12-1	180	270	235	253	500	13/0.20	2.0	87.01	74.85	0.86	83.63	0.96
R12-2				253				83.28	74.85	0.90	83.63	1.00
R13-1				380				97.52	88.70	0.91	97.33	1.00
R13-2				380				106.56	88.70	0.83	97.33	0.91
R14-1				507				116.50	102.41	0.88	110.90	0.95
R14-2				507				116.84	102.41	0.88	110.90	0.95
R22-1				253/253				107.00	97.24	0.91	105.73	0.99
R22-2				253/253				105.71	97.24	0.92	105.73	1.00
R23-2				380/380				131.65	121.72	0.92	129.93	0.99
									Mean:	0.89		0.97
Chen et al. (2018), f_c' = 141.5 MPa, σ_t = 12.0 MPa												
B-1	150	220	188	308	461	13/0.20	2.0	43.30	49.81	1.15	54.30	1.25
B-2			184	760	417			71.40	77.00	1.08	81.07	1.14
B-3			182	982	456			90.40	95.81	1.06	99.56	1.10
B-4			182	982/360	456			105.90	114.95	1.09	117.37	1.11
									Mean:	1.10		1.15
Yoo et al. (2017), f_c' = 197 MPa, σ_t = 10.9 MPa												
UH-0.53	200	270	240	253	523	13/0.20	2.0	97.91	82.09	0.84	86.65	0.88
UH-1.06				507				118.65	111.66	0.94	116.09	0.98
UH-1.71				380				130.99	133.64	1.02	137.93	1.05
									Mean:	0.93		0.97
Hasgul et al. (2018), f_c' = 162 MPa, σ_t = 9.32 MPa												
B1-F	150	250	223	308	453	13/0.16	1.5	52.59	60.06	1.14	60.05	1.14
B2-F			220	628	463			89.76	89.87	1.00	89.85	1.00
B3-F			218	905	456			111.91	111.73	1.00	111.72	1.00
B4-F			220	628/628	465			134.35	132.39	0.99	132.39	0.99
									Mean:	1.03		1.03
Turker et al. (2019), f_c' = 163 MPa, σ_t = 11.18 MPa												
K1-F	150	250	223	308	445	13/0.16	1.0	51.31	61.39	1.20	65.34	1.27
K2-F			220	628	471	60/0.75	0.5	88.61	91.49	1.03	95.08	1.07
K3-F			218	905	460			106.29	114.24	1.07	117.73	1.11
K4-F			220	628/628	471			127.60	134.97	1.06	138.23	1.08
									Mean:	1.09		1.13
									Mean:	0.99		1.04
									Std :	0.10		0.10
									CoV :	0.11		0.09

Reinforced Concrete (UHPFRC) beams produced in mono and hybrid forms were investigated experimentally and numerically. For this purpose, total of twelve doubly reinforced concrete beams were produced for different reinforcement ratios which represent low to excessive levels (ρ = 0.009, 0.019, 0.028 and 0.043). The test beams were subjected to the four-point loading and the results were discussed below in terms of the many parameters. In addition to the test program, two numerical approaches were proposed to predict nominal moment capacity of the UHPFRC beams in the mono or hybrid form. The approaches were applied to the current test beams and various UHPFRC beams previously studied in the literature.

- The deflection ductility of non-fiber beams decreased from 8.14 to 2.11 with increasing of the tensile reinforcement ratio. Although the deflection ductility for the mono UHPFRC beam decreased 2.3 times in comparison to the non-fiber beam with the lowest reinforcement ratio, the ductility values and fibers' effectiveness significantly increased as the reinforcement ratio increases. In a similar manner, the ductility values for the hybrid beams showed an increasing trend with the reinforcement ratio. It can be noted that the ductility values of the hybrid fiber beams are greater than those of the mono use for each reinforcement ratio. The highest ductility among the test beams was achieved for the beams with the reinforcement ratio of 0.028. This ratio is well above the limits in the current design codes. From the curvature measurements, overly high curvature ductilities were obtained for the test beams due to the formation of major crack. The maximum curvature ductilities were obtained for the highest reinforcement ratio (ρ = 0.043).
- Since no confinement effect was provided by the stirrups in the mid-region of beams, the reinforcement buckling was observed shortly after the concrete crushing in the non-fiber beams with low reinforcement ratios. Due to the effectiveness of steel fibers with respect to the confinement, despite the concrete crushing, the concrete cover remained intact and the fibers did not allow buckling in the case of UHPFRC beams for same reinforcement ratios.
- While a significant flexural stiffness increase was obtained for the mono and hybrid UHPFRC beams with the lowest reinforcement ratio, this change remained limited for the further ratios. However, the flexural stiffnesses of the mono fiber beams were slightly more than the hybrid beams for all reinforcement ratios due to the fiber content considered in the mixture.
- The UHPFRC use provides additional moment capacities through the contribution of fibers in the compression and tension regions in comparison with the non-fiber conditions. As the tensile reinforcement ratio increases, the fiber contribution on the capacity decreased for both fiber usages. Noted that the moment capacities of hybrid beams are slightly smaller than the mono beams since the volumetric ratio of short fiber in the hybrid mixture is less and it governs the strength and stiffness responses beams prior to the cracking.

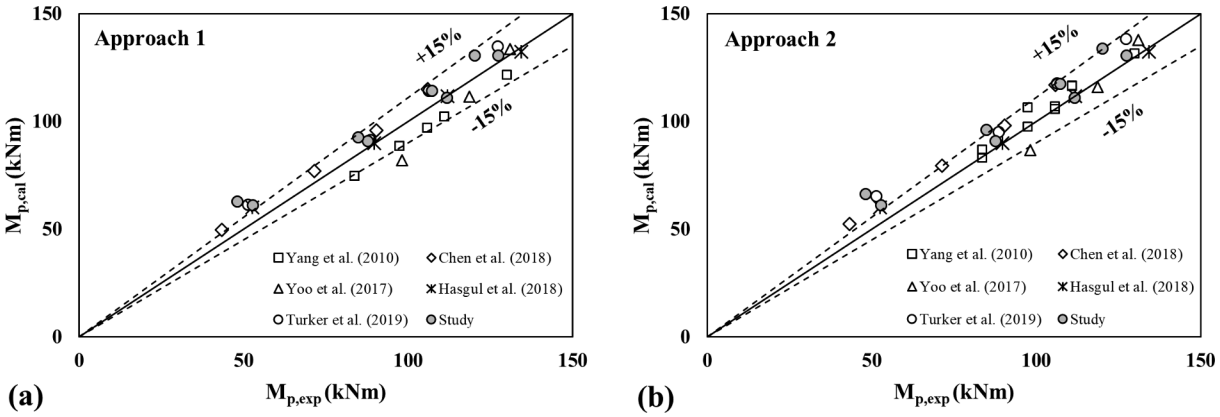

Fig. 18. Comparisons of the calculated and experimental moment capacities; a) Approach 1, b) Approach 2.

- The test results also showed that the cracking behaviors were affected differently by the fiber usage at the serviceability (SLS) and ultimate limit states (ULS). The total number of cracks in the mono fiber beams for the SLS significantly decreased and this fiber usage limited the crack widths in comparison with the non-fiber condition. However, the hybrid beams could not show good performance comparing to others because the long fibers in the matrix are not already activated to limit the cracks. The authors think that if more short fiber in the hybrid concrete mixture would be considered, better cracking behavior could be achieved for this limit state. On the other hand, for the ULS after the peak load, the hybrid fiber usage significantly limited to the crack widths for especially higher reinforcement ratios since the most of short fibers already pulled out and the long fibers in the concrete matrix were activated.
- It was observed that the characteristic responses of compressive strains are regardless of the reinforcement ratio and fiber usage. While an average concrete strain of 0.0033 was obtained for the non-fiber beams, this value was nearly 0.004 for the mono and hybrid UHPFRC beams.
- The proposed numerical approaches, in which the first one uses many fiber parameters in the UHPFRC matrix and other uses the direct tensile test result to determine the tensile strength of the concrete in mono or hybrid form, were applied to the doubly reinforced test beams. The calculated numerical capacities are in good agreement with the test results for the reinforcement ratio of 1.9% and above, but they can overestimate the capacities for the lowest reinforcement ratio. The approaches were also applied to the total of 24 singly reinforced UHPFRC beams previously studied in the literature. It is evident from these results that both approaches can be sufficiently determine the moment capacities within a band of ± 15% even though dimensions, reinforcement ratios, yield strengths and compressive/tensile behaviors are quite different and they were produced probable different casting techniques.

The current results presented in the study show that the use of UHPFRC provides remarkable benefits in terms of ductility, flexural capacity, stiffness and cracking control. However, higher reinforcement ratios above the well-known design limits can be used to benefit from the UHPFRC's excellent compressive and deformation capacities. This can allow the production of slender members having higher load-carrying capacity. Hence, more aesthetic, economic and long-lasting design applications can be possible with the UHPFRC use. It should be also noted that the hybrid fiber usage in the UHPFRC may allow more efficiency in terms of flexural behavior.

6. Data availability

The raw/processed data required to reproduce these findings cannot be shared at this time as the data also forms part of an ongoing study.

References

[1] Graybeal BA. Flexural behavior of an ultrahigh-performance concrete I-girder. J Bridge Eng 2008;13(6):602–10.
[2] Wille K, Naaman AE, Parra-Montesinos GJ. Ultra-high performance concrete with compressive strength exceeding 150 MPa (22 ksi): a simpler way. ACI Mater J 2011;108(1):46–54.
[3] SAMARIS, Report D22, Full scale application of UHPFRC project rehabilitation of bridges-from the lab to the field, European project 5th FWP/SAMARIS-Sustainable and Advanced Materials for Road Infrastructures-WP 14: HPFRCC, 2005.
[4] Moreillon L, Menétrey P. Rehabilitation and strengthening of existing rc structures with uhpfrc: various application. In: RILEM-fib-AFGC Int. Symposium on Ultra-High Performance Fibre-Reinforced Concrete, France, RILEM Publication S. A. R. L, Marseille, 1-2 October 2013. p. 127-136.
[5] Guan Q, Zhang P, Xie X. Flexural behavior of steel fiber reinforced high-strength concrete beams. Res J Appl Sci, Eng Technol 2013;6(1):1–6.
[6] Yang IH, Joh C, Kim BS. Structural behavior of ultra high performance concrete beams subjected to bending. Eng Struct 2010;32(11):3478–87.
[7] Yoo DY, Yoon YS. Structural performance of ultra-high-performance concrete beams with different steel fibers. Eng Struct 2015;102:409–23.
[8] Yoo DY, Banthia N, Yoon YS. Experimental and numerical study on flexural behavior of UHPFRC beams with low reinforcement ratios. Can J Civ Eng 2017;44(1):18–28.
[9] Dancygier AN, Berkover E. Cracking localization and reduced ductility in fiber-reinforced concrete beams with low reinforcement ratios. Eng Struct 2016;111:411–24.
[10] Deluce JR, Vecchio FJ. Cracking behavior of steel fiber-reinforced concrete members containing conventional reinforcement. ACI Struct J 2013;110(3):481–90.
[11] Yuguang Y, Walraven JC, Uijl JA. Combined effect of fibers and steel rebars in high performance concrete. Heron 2009;54(2/3):205–24.
[12] Dancygier AN, Savir Z. Flexural behavior of HSFRC with low reinforcement ratios. Eng Struct 2006;28:1503–12.
[13] Wille K, Naaman AE, El-Tawil S, Parra-Montesinos GJ. Ultra-high performance concrete and fiber reinforced concrete: achieving strength and ductility without heat curing. Mater Struct 2012;45:309–24.
[14] Kim DJ, Park SH, Ryu GS, Koh KT. Comparative flexural behavior of hybrid ultra high performance fiber reinforced concrete with different macro fibers. Constr Build Mater 2011;25:4144–55.
[15] Wille K, Parra-Montesinos GJ. Effect of beam size, casting method, and support conditions on flexural behavior of ultra-high-performance fiber-reinforced concrete. ACI Mater J 2012;379–388.
[16] Yoo DY, Lee JH, Yoon YS. Effect of fiber content on mechanical and fracture properties of ultra high performance fiber reinforced cementitious composites. Compos Struct 2013;106:742–53.
[17] Yoo DY, Kang ST, Yoon YS. Effect of fiber length and placement method on flexural behavior, tension-softening curve, and fiber distribution characteristics of UHPFRC. Constr Build Mater 2014;64:67–81.
[18] Yoo DY, Shin HO, Yang JM, Yoon YS. Material and bond properties of ultra high performance fiber reinforced concrete with micro steel fibers. Compos B 2014;58:122–33.
[19] Yoo DY, Banthia N, Yoon YS. Predicting the flexural behavior of ultra-high-performance fiber-reinforced concrete. Cem Concr Compos 2016;74:71–87.
[20] Yazıcı H, Deniz E, Baradan B. The effect of autoclave pressure, temperature and duration time on mechanical properties of reactive powder concrete. Constr Build Mater 2013;42:53–63.
[21] Yazıcı H, Yardımcı MY, Yigiter H, Aydın S, Türkel S. Mechanical properties of reactive powder concrete containing high volumes of ground granulated blast furnace slag. Cem Concr Compos 2010;32:639–48.
[22] Kahanji C, Ali F, Nadjai A. Structural performance of ultra-high-performance fiber-reinforced concrete beams. Struct Concr 2017;18(2):249–58.
[23] Chen L, Graybeal BA. Modeling structural performance of second-generation ultrahigh-performance concrete pi-girders. J Bridge Eng 2012;17(4):634–43.
[24] Yang IH, Joh C, Kim BS. Flexural strength of large-scale ultra high performance

concrete prestressed T-beams. Can J Civ Eng 2011;38:1185–95.
[25] Qi J, Wang J, John Z. Flexural response of high-strength steel-ultra-high-performance fiber reinforced concrete beams based on a mesoscale constitutive model: experiment and theory. Struct Concr 2018;19(3):719–34.
[26] Chen S, Zhang R, Jia LJ, Wang JY. Flexural behaviour of rebar-reinforced ultra-high-performance concrete beams. Magn Concr Res 2018;70(19):997–1015.
[27] Yoo DY, Banthia N, Yoon YS. Flexural behavior of ultra-high-performance fiber-reinforced concrete beams reinforced with GFRP and steel rebars. Eng Struct 2016;111:246–62.
[28] Singh M, Sheikh AH, Ali MSM, Visintin P, Griffith MC. Experimental and numerical study of the flexural behaviour of ultra-high performance fibre reinforced concrete beams. Constr Build Mater 2017;138:12–25.
[29] Kamal MM, Safan MA, Etman ZA, Salama RA. Behavior and strength of beams cast with ultra high strength concrete containing different types of fibers. HBRC J 2014;10:55–63.
[30] Shafieifar M, Farzad M, Azizinamini A. A comparison of existing analytical methods to predict the flexural capacity of Ultra High Performance Concrete (UHPC) beams. Constr Build Mater 2018;172:10–8.
[31] Tanarslan HM, Alver N, Jahangiri R, Yalçınkaya Ç, Yazıcı H. Flexural strengthening of RC beams using UHPFRC laminates: bonding techniques and rebar addition. Constr Build Mater 2017;155(30):45–55.
[32] Hasgul U, Turker K, Birol T, Yavas A. Flexural behavior of ultra-high-performance fiber reinforced concrete beams with low and high reinforcement ratios. Struct Concr 2018;19(6):1577–90.
[33] Turker K, Birol T, Yavas A, Hasgul U, Yazici H. Flexural behavior of beams with ultra high performance fiber reinforced concrete. Tech J 2019;30(1):8777–801.
[34] Rossi P, Antonio A, Parant E, Fakhri P. Bending and compressive behaviors of a new cement composite. Cem Concr Res 2005;35(1):27–33.
[35] Wille K, Kim DJ, Naaman AE. Strain-hardening UHP-FRC with low fiber contents. Mater Struct 2011;44(3):583–98.
[36] Banthia N, Sappakittipakorn M. Toughness enhancement in steel fiber reinforced concrete through fiber hybridization. Cem Concr Res 2007;37(9):1366–72.
[37] Sorelli LG, Meda A, Plizzari GA. Bending and uniaxial tensile tests on concrete reinforced with hybrid steel fibers. J Mater Civ Eng 2005;17(5):519–27.
[38] Akcay B, Tasdemir MA. Mechanical behaviour and fibre dispersion of hybrid steel fibre reinforced self-compacting concrete. Constr Build Mater 2012;28(1):287–93.
[39] Banthia N, Nandakumar N. Crack growth resistance hybrid fiber reinforced cement composites. Cem Conc Comp 2003;25(1):3–9.
[40] Banthia N, Gupta R. Hybrid fiber reinforced concrete (HyFRC): fiber synergy. Mater Struct 2004;37(10):707–16.
[41] Nehdi M, Ladanchuk JD. fiber synergy in fiber-reinforced self-consolidating concrete. ACI Mater J 2004;101(6):508–17.
[42] Ahmed SFU, Maalej M, Paramasivam P. Flexural responses of hybrid steel-polyethylene fiber reinforced cement composites containing high volume fly ash. Constr Build Mater 2007;21(5):1088–97.
[43] Sivakumar A, Santhanam M. Mechanical properties of high strength concrete reinforced with metallic and non-metallic fibres. Cem Conc Comp 2007;29(8):603–8.
[44] Dawood ET, Ramli M. Mechanical properties of high strength flowing concrete with hybrid fibers. Constr Build Mater 2012;28(1):193–200.
[45] Sivakumar A, Santhanam M. A quantitative study on the plastic shrinkage cracking in high strength hybrid fibre reinforced concrete. Cem Conc Comp 2007;29(7):575–81.
[46] Cao M, Zhang C, Lv H. Mechanical response and shrinkage performance of cementitious composites with a new fiber hybridization. Constr Build Mater 2014;57:45–52.
[47] Yıldırım G. Dimensional stability of deflection-hardening hybrid fiber reinforced concretes with coarse aggregate: suppressing restrained shrinkage cracking. Struct Conc 2019;20(2):836–50.
[48] Afroughsabet V, Ozbakkaloglu T. Mechanical and durability properties of high-strength concrete containing steel and polypropylene fibers. Constr Build Mater 2015;94:73–82.
[49] Li Y, Tan KH, Yang E-H. Influence of aggregate size and inclusion of polypropylene and steel fibers on the hot permeability of ultra-high performance concrete (UHPC) at elevated temperature. Constr Build Mater 2018;169:629–37.
[50] Li Y, Pimienta P, Pinoteau N, Tan KH. Effect of aggregate size and inclusion of polypropylene and steel fibers on explosive spalling and pore pressure in ultra-high-performance concrete (UHPC) at elevated temperature. Cem Concr Comp 2019;99:62–71.
[51] Yang IH, Joh C, Kim BS. Flexural response predictions for ultra-high-performance fibre-reinforced concrete beams. Mag Concr Res 2012;64(2):113–27.
[52] Khalil W, Tayfur YR. Flexural strength of fibrous ultra high performance reinforced concrete beams. ARPN J Eng Appl Sci 2013;8(3):200–14.
[53] Imam M, Vandewalle L, Mortelmans F. Shear-moment analysis of reinforced high strength concrete beams containing steel fibres. Can J Civ Eng 1995;22(3):462–70.
[54] Xia J, Chanb T, Mackieb KR, Saleemc MA, Mirmiran A. Sectional analysis for design of ultra-high performance fiber reinforced concrete beams with passive reinforcement. Eng Struct 2018;160:121–32.
[55] JSCE. Recommendations for Design and Construction of High Performance Fiber Reinforced Cement Composites with Multiple Fine Cracks (HPFRCC). Japanese Society of Civil Engineers: Tokyo, Japan, 2008.
[56] AFGC, Interim Recommendations, Ultra High Performance Fibre Reinforced Concretes, France, 2013.
[57] Fehling E, Schmidt M, Walraven J, Leutbecher T, Fröhlich S. Ultra-High Performance Concrete UHPC: Fundamentals, Design, Examples. Ernst & Sohn, Berlin, Germany, 2014.
[58] FHWA (Federal Highway Administration) FHWA-HRT-06-103: Material Property Characterization of Ultra-High Performance Concrete. FHWA, Washington, DC, USA, 2006.
[59] TS 500. Requirements for Design and Construction of Reinforced Concrete Structures, Ankara, Turkish Standards Institution, 2000 (in Turkish).
[60] Park R. Evaluation of ductility of structures and structural assemblages from laboratory testing. Bull New Zealand Natl Soc Earthq Eng 1989;22(3):155–66.
[61] ACI Committee 544. Design Consideration for Steel Fiber Reinforced Concrete (ACI 544.4R-88), American Concrete Institute, Farmington Hills, MI, 2009.
[62] Lim TY, Paramasivam P, Lee SL. Shear and moment capacity of reinforced steel fiber concrete beams. Magn Concr Res 1987;39(140):148–60.
[63] Bae BI, Choi HK, Choi CS. Flexural strength evaluation of reinforced concrete members with ultra high performance concrete. Adv Mater Sci Eng 2016;2815247:1–10.
[64] Naaman E, Najm H. Bond-slip mechanisms of steel fibers in concrete. ACI Mater J Proc 1991;88(2):135–45.
[65] Al-Ta'an SA, Al-Feel JR. Evaluation of shear strength of fibre-reinforced concrete beams. Cem Conc Compos 1990;12(2):87–94.
[66] Ahmed HI, Pama RP. Ultimate flexural strength of reinforced concrete beams with large volumes of short randomly oriented steel fibres. In: Fibre reinforced cement and concrete: proceedings of the fourth international symposium held by Rilem, University of Sheffield, UK, Sheffield, 20-23, July 1992.
[67] Dwarakanath HV, Nagaraj TS. Deformational behavior of reinforced fiber reinforced concrete beams in bending. J Struct Eng 1992;118(10):2691–8.
[68] Oh BH. Flexural analysis of reinforced concrete beams containing steel fibers. J Struct Eng 1992;118(10):2821–36.